

GRANITE VISION: A LIGHTWEIGHT, OPEN-SOURCE MULTIMODAL MODEL FOR ENTERPRISE INTELLIGENCE

Granite Vision Team, IBM Research

See Contributions and Acknowledgments section for full authors list

granite-inquiries@ibm.com

ABSTRACT

We introduce Granite Vision, a lightweight large language model with vision capabilities, specifically designed to excel in enterprise use cases, particularly in visual document understanding. Our model is trained on a comprehensive instruction-following dataset, including document-related tasks, such as content extraction from tables, charts, diagrams, sketches, and infographics, as well as general image tasks. The architecture of Granite Vision is centered around visual modality alignment with a decoder-only, 2 billion-parameter Granite large language model. Additionally, we introduce a dedicated safety classification approach in test-time that leverages a sparse set of attention vectors to identify potential harmful inputs. Despite its lightweight architecture, Granite Vision achieves strong results in standard benchmarks related to visual document understanding, as well as on the LiveXiv benchmark, which is designed to avoid test set contamination by using a constantly updated corpus of recently published Arxiv papers. We are releasing the model under the Apache-2 license, allowing for both research and commercial use, while offering complete visibility into the training data and other relevant details. See <https://huggingface.co/ibm-granite/> for model weights.

1 INTRODUCTION


The confluence of computer vision and natural language processing has led to significant advances in multimodal learning, enabling large language models to effectively integrate and reason about visual content and linguistic data. Both proprietary and open-source multimodal models (Grattafiori et al., 2024; Team et al., 2024; OpenAI, 2023a; Abdin et al., 2024a; Dai et al., 2024; Zhang et al., 2024a; Wang et al., 2024; Agrawal et al., 2024; Li et al., 2024b; Chen et al., 2024b; Deitke et al., 2024a) have achieved remarkable success on a range of standard benchmarks, including visual question-answering, as well as more complex tasks such as multi-image reasoning and video understanding.

While this progress is exciting, a notable disparity remains: smaller models, typically with 1-4 billion parameters, have consistently fallen short of achieving performance comparable to their larger counterparts containing tens of billions of parameters. In addition, existing models are predominantly trained on natural images, which can limit their performance in other domains, such as visual document understanding, where the unique visual characteristics, such as layouts, fonts, and graphics, significantly differ from natural images and require a more fine-grained comprehension of the visual content.

In this work, we introduce Granite Vision, a compact vision-language model with approximately 3 billion parameters¹, tailored to excel in enterprise use cases. Although our model can process general images, the first version of Granite Vision is particularly focused on visual document understanding, enabling automated content extraction from tables, charts, infographics, plots, diagrams, sketches, and more. Figure 1 shows qualitative examples of our model’s output for visual document understanding tasks and general image description. Granite Vision extends the Granite family of large language models (Granite Team (2024)), which have been trained on more than 12 trillion tokens, achieving state-of-the-art performance for their size, while being designed for enterprise usage, with full visibility into the training data.

¹We denote our model as Granite-Vision-3.1-2B, where the version (3.1) and size (2B) of the base large language model are explicitly indicated. However, when considering the integrated vision encoder and projector, the total parameter count of our model increases to 3 billion parameters.

(a)



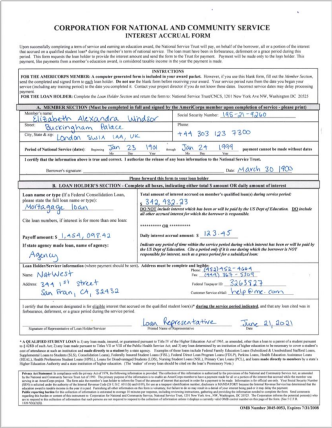
What is the total order price?

\$52.48

What has been ordered?

1 WINE BOTTLE, 2 CHEESE STEAK, 1 SPICY BARQUE STEAK

(b)



Describe the document in high level.

The document is an Interest Accrual Form for the National and Community Service Corporations. It outlines the process for accruing interest on a qualified student loan during a member's term of national service. The form requires the member to provide their personal information, loan details, and certify the accuracy of the information provided. The member must also authorize the release of loan information to the National Service Trust.


What is the name of the member that the form is filled in for?

The name of the member is Elizabeth Alexandra Windsor.

Is there a signature missing in the form?

Yes, the signature is missing in the form.

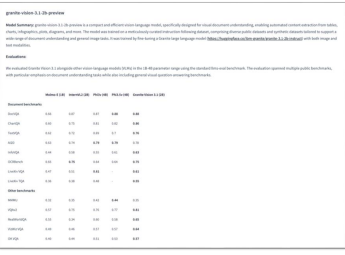
(c)



Describe the scene in this image.

The image depicts a scene of a car accident. There is a damaged vehicle with its front end severely damaged, with the hood crumpled and the front wheel detached. The car is parked on a street, and there are some trees and buildings in the background. Two individuals are present in the scene, one of whom is a man wearing a high-visibility vest and the other is a woman. The man is kneeling down and appears to be examining the damage to the car, while the woman is crouching beside him, looking at the damage. The man is holding a tablet in his hand, possibly taking notes or looking up information about the damage. The woman is wearing a striped shirt and jeans. The overall atmosphere of the image suggests that the individuals are assessing the damage to the car and possibly discussing the next steps in the aftermath of the accident.

(d)



What is the highest scoring model on ChartQA and what is the score?

The highest scoring model on ChartQA is Granite Vision 3.1 with a score of 0.86.

Figure 1: Qualitative examples generated by Granite Vision, showcasing its diverse capabilities including (a) document understanding such as receipt calculation, (b) form understanding with human handwritten text, (c) knowledge-grounded image description, (d) table understanding, etc.

As a key contribution of our work, we meticulously curate a comprehensive instruction-following dataset for visual document understanding, comprising around 13 million images and 80 million instructions, which span a diverse set of tasks, including document question-answering, scene text understanding, key-value extraction, text grounding, layout parsing, captioning, UI understanding, and code (see Figure 2). We constructed this dataset by (i) mining documents from the web and synthesizing instructions as described in Section 3.1, and (ii) unifying multiple public datasets into a single format. In addition to documents, our training data is further enriched by the inclusion of instruction-following data for general images from public datasets (Tong et al., 2024; Li et al., 2024b; Laurençon et al., 2024b; Liu et al., 2023b).

Similar to LLaVA (Liu et al., 2023c), our approach uses a projector to establish a connection between the visual encoder and a Granite large language model. Our training protocol consists of multiple stages, progressing from training the projector in isolation to jointly fine-tuning both the projector and the large language model, using denser image resolution grids at the latest stages. We also extract multi-layer features from the encoder, allowing us to better capture fine-grained details that are important for visual document understanding. Finally, we propose a novel method for safety classification as a separate module to identify harmful inputs based on a sparse set of attention vectors, which are selectively chosen to maximize safety classification performance.

Compared to other models of similar parameter size, Granite Vision achieves state-of-the-art results on established benchmarks for visual document understanding, conversion of tables and charts to structured formats, and the LiveXiv benchmark (Shabtay et al., 2024), which evaluates the model on recently published Arxiv papers, helping to mitigate the risk of test set contamination that can arise when models are trained on web-scraped data. In addition to its strong performance in enterprise settings, our model demonstrates competitive results on standard vision-language benchmarks. To promote openness and collaboration, we make the model publicly available under the Apache-2 license, allowing visibility into the training data and procedures.

2 RELATED WORK

2.1 MULTIMODAL LARGE LANGUAGE MODELS

Recent advances in multimodal large language models (MLLMs) have demonstrated significant progress in understanding and generating content across different data modalities. Comprehensive surveys by Yin et al. (2024) and Wadekar et al. (2024) closely outline the various approaches to architecture design, training strategies, and evaluation methodologies in the field. The introduction of Flamingo (Alayrac et al., 2022) highlighted a remarkable performance of the transformer cross-attention architecture in vision-language tasks, serving as a catalyst for further advancements in the multimodal domain. The launch of GPT-4V (OpenAI, 2023b) has sparked a competitive race in the development of powerful commercial-use MLLMs, leading to multimodal models like GPT-4o (OpenAI, 2024), Claude 3.5 Sonnet (Anthropic, 2024), and Gemini Pro 1.5 (Team et al., 2024). In parallel, the open-source community has made significant contributions, with models like BLIP2 (Li et al., 2023), Phi-3.5-vision (Abdin et al., 2024b), LLaVA-OneVision (Li et al., 2024c), and Llama 3.2-vision (Grattafiori et al., 2024) showing competitive performance on benchmarks while maintaining transparency and accessibility. To mitigate the high costs associated with training large models in an end-to-end manner, a common approach involves employing modular architectures. These architectures typically combine a pre-trained modality encoder and a pre-trained large language model (LLM) with a learnable modality connector, with the latter comprising only a small portion of the total parameters (Bai et al., 2023; Tong et al., 2024; Chen et al., 2024b). More recently, Zhang et al. (2024a) demonstrated that even relatively small models can achieve strong performance with careful data curation and optimized training strategies. Building on these insights, our model uniquely achieves state-of-the-art results on standard document and other benchmarks, all while operating at a significantly reduced scale (around 3 billion parameters).

2.2 VISUAL DOCUMENT UNDERSTANDING

Visual document understanding, particularly the ability to comprehend charts, diagrams, tables, and document images, represents a crucial application area for MLLMs. Two primary technical challenges emerge in enabling MLLMs to process documents and associated images effectively: adequately encoding high-resolution images, and accurately interpreting visually-situated text within the documents. Recent approaches to addressing these challenges are often broadly categorized into two groups based on their text recognition methodology. The first category, including models like DocFormer (Appalaraju et al., 2021), LayoutLMv3 (Huang et al., 2022), and, more recently, DocLLM (Wang et al., 2023), relies on external optical charac-

ter recognition (OCR) systems to process text within images. The second category consists of “OCR-free” models, e.g. Donut (Kim et al., 2022b), UReader (Ye et al., 2023), mPLUG-DocOwl 1.5 (Hu et al., 2024a), and DocPedia (Feng et al., 2024). Besides the specialized multimodal document understanding models (Liao et al., 2024; Liu et al., 2024a), strong performance is also achieved by general MLLMs instruction-tuned on document datasets (Li et al., 2024c; Dai et al., 2024). While recent efforts (Mathew et al., 2021; HuggingFace, 2025; Rodriguez et al., 2024) have produced several open-source document understanding datasets to advance model performance in this domain, large comprehensive datasets without restrictive licensing remain relatively limited. Our approach builds upon this foundation by leveraging a comprehensive instruction-following dataset for visual document understanding, incorporating both synthetic data and public datasets.

3 DATA

Granite Vision has been trained on a comprehensive instruction-following dataset, which covers a wide variety of visual categories ranging from document images to general images. The training data consists of a combination of pre-curated public vision datasets, common-crawl PDFs, and data that is synthesized in-house. A detailed view of our data is presented in Figure 2, which depicts document understanding datasets, and Figure 3, which represents general image datasets. Our document understanding data (Figure 2) covers a variety of document classes such as general document images, charts, flowcharts, diagrams and several more encompassing a diverse set of visual Q&A tasks. See Table 5 (in Appendix) for a comprehensive overview of the datasets. Such diverse data is chosen to ensure the model’s ability to generalize across a wide array of document-centric applications. In addition to document datasets, we incorporated training data from multiple publicly available generic image datasets (Figure 3). In the following sections, we dive deep into different data categories, data collection processes, synthetic data generation techniques, and data pre-processing pipelines.

3.1 IBM CURATED DATASETS

In this section, we will describe several large synthetic document Q&A datasets created at IBM and focused on a diverse set of document and Q&A tasks. In order to seed this effort, we leveraged DocFM, a large-scale comprehensive dataset effort at IBM consisting of 85 million document pages extracted from unique PDF documents sourced from Common Crawl, Wikipedia, and ESG (Environmental, Social, and Governance) reports. DocFM served as a foundation for generating our synthetic datasets, which capitalized on its enriched nature for granular filtering and balancing.

DocFM was created using Docling (Livathinos et al., 2025), an open-source document conversion toolkit developed by IBM. Docling facilitated the extraction and enrichment of each page with a rich set of attributes, resulting in a highly detailed representation of document pages. Specifically, this enabled:

- **Text and Positional Metadata Extraction:** Parsing each PDF page to retrieve textual content along with its positional metadata.
- **Layout Understanding:** Identification of structural components such as headers, footers, paragraphs, lists, captions, code, formulas, form elements, pictures, footnotes, and document indices.
- **Reading Order Detection:** Establishing the reading sequence of extracted content based on layout and parsed output.
- **Language Detection:** Identifying the primary language present on each page.
- **Figure Classification:** Labeling visual elements, such as charts, images, and diagrams.

To ensure high-quality textual representation, we focused exclusively on PDFs with extractable content, ensuring reliable and efficient text processing while minimizing noise.

3.1.1 DOCFM - DATA COLLECTION & FILTERING

A large portion of the DocFM dataset was obtained from the Common Crawl corpus which is an open repository of web data. It is freely accessible and distributed as monthly archive files in various formats (“segments”). Among these segments, the URL index contains a list of crawled URLs accompanied by metadata, such as the media type specified by the HTTP header and the media type detected by Common Crawl from the actual URL content. By adhering to the Robots Exclusion Protocol (Koster et al., 2022) (commonly known as

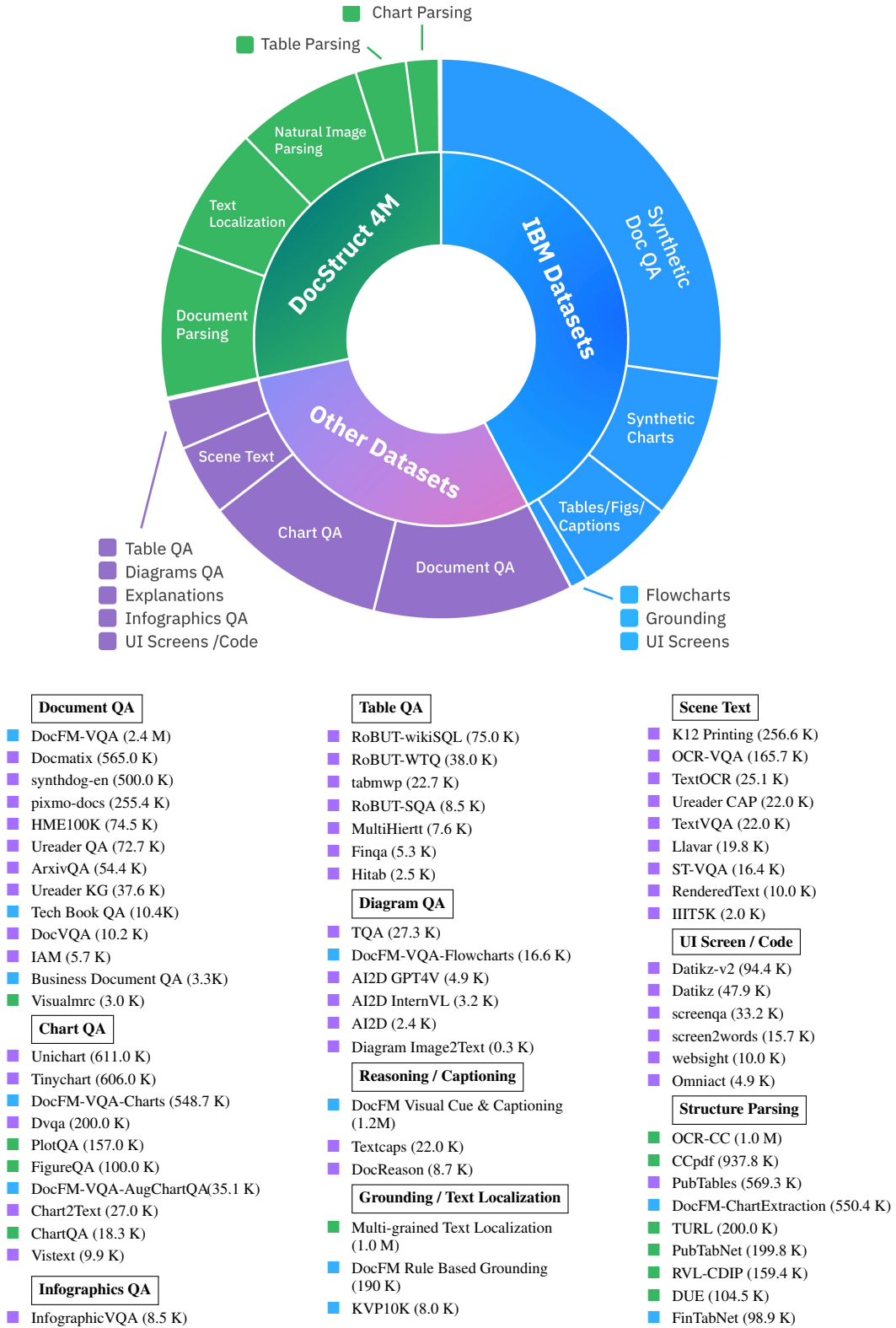


Figure 2: Overview of our comprehensive collection of document understanding datasets used for Granite Vision training.

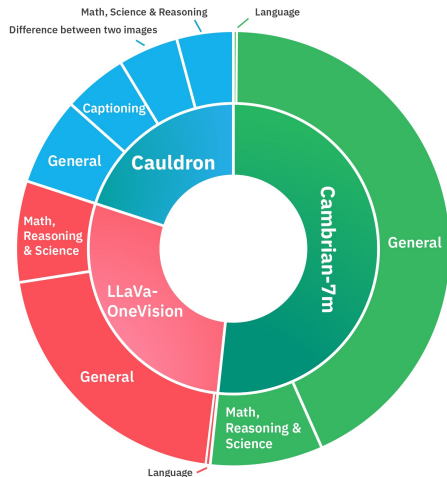


Image Count per Category Across Datasets

	Cauldron	LLaVa-OneVision	Cambrian-7m
General	276.5 K	881.3 K	1.8 M
Language/Captioning	202.1 K	N/A	N/A
Math/Science/Reasoning	178.4 K	318.0 K	354.5 K
Image Comparison	188.9 K	N/A	N/A

QA Count per Category Across Datasets

	Cauldron	LLaVa-OneVision	Cambrian-7m
General	812.7 K	2.0 M	7.9 M
Language/Captioning	203.3 K	1.2 M	1.8 M
Math/Science/Reasoning	765.1 K	464.8 K	802.0 K
Image Comparison	237.9 K	N/A	N/A

Figure 3: Overview of general image datasets used for Granite Vision training.

“robots.txt”), Common Crawl ensures basic operational guarantees. We obtained the Common Crawl dataset partition through the following process:

- A set of trusted web domains likely to contain relevant PDF files was manually curated. Additionally, websites of affiliations from public GitHub² repositories, primarily universities and educational institutions, were identified. In total, we cataloged more than 45,000 domains to increase the relevance of the dataset and minimize potential issues related to web crawl data (e.g., toxic language, hate speech, abusive language, or profanity).
- For each domain in the curated list, a search was conducted across the Common Crawl index segments of 13 archives (spanning May 2021 to January/February 2023) to identify URLs with the media type “application/pdf,” as either declared or detected.
- For each discovered URL, we made an attempt to download the PDF file from the source. If successful, the file and its metadata were stored in a database.

Through this process, 4.96 million URLs were identified, resulting in 3.98 million PDF files after accounting for exact (binary) duplicates and invalid links. Additionally, we included 838,237 PDF documents retrieved from CCpdf (Turski et al., 2023a). After deduplicating, 4.6 million unique PDF files (75.5 million pages) remained in the Common Crawl partition. Following the conversion process, we successfully converted 65 million pages.

In addition, a total of 7,696 ESG reports were all sourced directly from Responsibility Reports³. To complement this, an automated pipeline using a headless Chrome browser component was employed to convert 20M pages of Wikipedia articles into PDF format. The list of articles was derived from the wikipedia dataset (Foundation).

DocFM is a very large dataset which we plan to use for a variety of downstream visual learning applications in the future. For the current release of Granite Vision, we focused on a subset of DocFM for creation of a family of synthetic visual QA datasets (LLM and rule-based document and chart VQA) which will be described next.

3.1.2 IBM SYNTHETIC VISUAL Q&A DATASETS

DocFM-VQA (Synthetic Document VQA): There’s a lack of large-scale instruction-following datasets focused on visually-rich document understanding. The most commonly used dataset, DocVQA (Mathew et al., 2021), is limited in size as it contains only 10K images and 40K QA pairs. Docmatix (HuggingFace, 2025) has been recently introduced as a potential large-scale alternative to DocVQA, but it uses only the textual parts of documents for QA pairs generation.

²<https://github.com/>

³www.responsibilityreports.com

In our work, we leverage a large language model (Mixtral 8x22B), to synthetically generate a large-scale visual question answering (VQA) dataset using a subset of DocFM as seed. We call this dataset DocFM verbalization-based VQA or DocFM-VQA in short. We employed a “verbalized” representation of the documents as context for the LLM’s (Mixtral 8x22B) QA generation. This involved extracting text from programmatic PDFs and augmenting it with verbal descriptions of visual elements such as charts, images, and tables. This approach encouraged the generation of questions that specifically target these elements. Our verbalization process included: 1) Converting charts to tables using DePlot (Liu et al., 2023a), 2) Replacing images with captions generated by BLIP2 (Li et al., 2023). 3) Converting tables to markdown format using TableFormer (Nassar et al., 2022). The DocFM-VQA contains a total of 20 million QA pairs from 2.4 million randomly selected pages from the DocFM dataset. This dataset facilitates the training of models capable of robust performance on visually rich documents. While we explored the use of leading Visual Language Models (VLMs) to filter out potential hallucinations in the generated QAs, the observed performance benefits did not outweigh the computational cost. Therefore, filtering was not incorporated into the current model version.

DocFM-VQA-charts (Synthetic Chart VQA): A general framework for synthetic QA generation on charts is to use tabular data in textual form, using an LLM to generate QAs on it, and using code to generate the appropriate visual chart. However, we observed two main issues with this approach. First, the generated QAs are unable to refer to visual properties like the used markers or plot colors. Second, LLMs tend to generate simple questions, such as a single data point extraction. As a result, large-scale synthetic chart QA datasets tend to dramatically improve the performance on synthetically generated benchmarks but have a smaller effect on human questions or human-annotated benchmarks (e.g. ChartQA’s augmented vs. human splits).

In our work, we addressed the two issues mentioned above by augmenting the tabular form of the data, used as input to the LLM for generating QAs, with additional information. To solve the first issue of the LLM lacking knowledge of the visual appearance of the chart, we first choose a random marker and color for each data sequence. This information is added to the table consumed by the LLM and provided as input to the code used for rendering the chart. To solve the second issue (of very simplistic QAs), we added to each table additional rows and columns. These rows and columns contain additional information calculated based on the original table using code. It includes max, min, sum, average, and a random operation (addition or subtraction) between two randomly chosen columns/rows, e.g. “Column 1 + Column 3”. This pre-calculated information encourages the model to ask questions requiring higher-order reasoning. It also allows the model to produce more accurate ground-truth answers for cases that require arithmetic capabilities that LLMs struggle with (Schwartz et al., 2024).

We used the augmented table approach as input to the DocFM-VQA pipeline to generate the DocFM-VQA-Charts dataset. It contains 5.5M QAs on about 500K synthetic charts rendered based on random numeric tables extracted from the DocFM dataset. We additionally augmented the ChartQA training set with the pre-calculated columns and rows information (without markers and colors) and generated additional QAs for the dataset’s existing images.

DocFM-VQA-flowcharts (Synthetic Flowchart VQA): In order for the model to better understand flowcharts we generated synthetic flowcharts with QA pairs. We used an LLM (Mixtral 8x7B) for generating the flowchart nodes and edges. We then use those nodes and edges to query an LLM for QA pairs and to render a visual representation of the flowchart. We used the pipeline described below to generate 17K JSON representation and rendered flowcharts. The JSONs are fed to the DocFM-VQA pipeline to generate 76K QA pairs.

The flowchart synthesis pipeline:

- *Identify Business Domains and Industries:* Utilize the LLM to extract various business domains and identify industries associated with typical business processes.
- *List Business Process Types:* For each business domain and industry, use the LLM to generate a comprehensive list of business process types.
- *Generate Business Processes:* For each business process type, we employ the LLM to create multiple business processes constructed in a JSON format. Each process should have nodes and edges, with the number of nodes ranging from 5 to 20.
- *Create Flowchart Images:* For each generated business process, use the ‘graphviz’ package to create a flowchart image. Incorporate random shapes, arrows, and colors to enhance visual diversity.

DocFM-ChartExtraction: We created a training dataset of 550K chart images to ensure that the model can perform structured data extraction from chart visualizations. The dataset was generated by converting tables extracted from DocFM and public stock market data into diverse chart types using matplotlib, including line, scatter, bar, pie, candlestick, and OHLC charts. For each visualization, training examples included extraction instruction with randomized output format requirements (Markdown, HTML, or JSON) and varied natural language phrasings. To enhance document-level understanding capabilities, 100K DocFM-derived charts were embedded into their source document contexts by covering the original table with the chart image. The financial subset comprises 40K candlestick and OHLC charts generated from NASDAQ, S&P500, and NYSE stock data. This synthetic dataset enables the training of vision-language models to extract structured information from diverse visualization types while handling multiple output formats and document contexts.

DocFM Visual Cue and Captioning: In order to create this dataset, we masked captions on images and then used the captions to generate questions regarding images. We implemented a multi-step process as follows: 1) Using Docling (Livathinos et al., 2025) we filtered to get figures associated with their corresponding captions; 2) We utilized Granite 3.1 8B model to analyze the captions for the presence of visual cues such as “black arrow,” “on the left,” “red circle,” and similar indicators of figure elements or regions of interest; 3) If the caption contained an explicit identifier (e.g., “Figure 5”), we extracted it using the parsed text from the PDF. The caption body text was then masked on the image, leaving only the identifier visible. If no explicit identifier was present, we used the figure’s bounding box as a fallback identifier. This identifier can then be used for the question, “*What is the black arrow pointing at in Figure 5.?*”. 4) Leveraging the LLM, we generated context-specific questions about the figure, using the caption to inform the question formulation and answer while hiding the textual context in the image.

DocFM Rule Based Grounding: We further complemented our data by implementing rule-based approaches to generate synthetic tasks focused on specific document elements like text localization, figures, and tables. Leveraging Docling’s layout detector (Pfzmann et al., 2022), we generated questions that query the location of text passages and other page elements. To encourage a deeper understanding of visual components, we masked captions associated with figures and tables, keeping only their identifiers. Subsequently, we employed templates to generate questions prompting the model to provide captions for these figures and tables. Furthermore, using defined templates we generated more operations such as selecting row, columns by index, or by value or comparison using only images. For the latter, we leverage the table understanding methods from Docling (Nassar et al., 2022; Lysak et al., 2023).

3.2 PUBLIC DATASETS

Our Granite Vision model is primarily focused on visual document understanding tasks. Therefore, we further enriched our data using a number of pre-curated high-quality, publicly available document-related datasets, which encompass several diverse tasks such as Document QA, Table QA, Chart QA, Diagram QA, OCR and scene-text related tasks, reasoning and grounding, UI screen/code and structure understanding. A detailed view of public document centric datasets is shown in Figure 2. For details readers are referred to Table 5 (in Appendix).

Beyond document-centric content, we also included high quality general image Q&As sourced from public datasets to ensure robust performance in general visual tasks as well. Specifically, we acquired data from three high-quality collections: Cauldron⁴, Cambrian-7M⁵ and LLaVa-OneVision-Data⁶. These datasets cover a wide range of domains and tasks, including image captioning, visual question answering (VQA), and object recognition, providing the foundational knowledge for general-purpose vision-language models. More details and statistics about general images data are shown in Figure 3.

3.3 DATA PREPROCESSING

Data pre-processing consisted of multiple annotation and filtering steps to conform to regulatory and safety requirements and improve overall data quality as described below.

⁴https://huggingface.co/datasets/HuggingFaceM4/the_cauldron

⁵<https://huggingface.co/datasets/nyu-visionx/Cambrian-10M>

⁶<https://huggingface.co/datasets/lms-lab/LLaVA-OneVision-Data>

- *Restricted Data removal*: All public datasets underwent a rigorous legal vetting process to identify data that could violate any legal or PII related requirements. All such data was removed, including datasets originating outside of the US and those with unclear license agreements.
- *Sexual Abuse Material (CSAM) removal*: All CSAM was removed from the datasets using state-of-the-art NSFW (not safe for work) detection methods.
- *Face blurring*: Face blurring was performed to obfuscate all visual PII from the data.
- *Deduplication*: Since we combined multiple dataset collections, there could be duplication of text as well as visual data. Similar images were detected through two methods: exact pixel-wise match, or perceptual hash matching (Zauner, 2010), for robustness against minor transformations. Records with identical texts *and* similar images were removed.

4 GRANITE VISION MODEL

In this section, we describe our model, including the architecture (Section 4.1), the training procedure (Section 4.2), and the use of Sparse Attention Vectors (SAVs) for safety classification (Section 4.3). An overview of our architecture is shown in Figure 4.

4.1 ARCHITECTURE

Vision-and-language models are designed to process two data modalities simultaneously, such as images and corresponding text instructions. Each modality is encoded into a shared embedding space, which is then utilized for reasoning by a language model f parameterized by θ . Specifically, an image is encoded using a pre-trained visual encoder, denoted as v parameterized by ϕ , and a projector M parameterized by λ . A corresponding textual prompt is tokenized and encoded using a fixed language encoder l parameterized by γ . Given an input image I and a text instruction P , the language model generates a text response R as follows: $R = f_{\theta}(M_{\lambda}(v_{\phi}(I)), l_{\gamma}(P))$. This section provides a detailed description of each of these components.

Vision Encoder v_{ϕ} . For an input image I , we use a vision encoder v_{ϕ} to provide visual features $X = v_{\phi}(I)$. In our implementation, X is a concatenation of outputs from multiple layers, allowing us to combine these different levels of representation, providing rich representations that are beneficial for visual document understanding. We use SigLIP (Zhai et al., 2023) as our vision encoder with 384×384 resolution. Additionally, we use the “AnyRes” technique in our training as in Li et al. (2024c), which is designed to accommodate images of various high resolutions. The ability to process high-resolution images is of particular importance for document understanding, especially when dealing with documents containing small text fonts, as it enables accurate text recognition.

Specifically, we use a global image, and a grid configuration that divides the image into multiple patches (or views), resulting in an additional multi-patch setting. We select the closest resolution from a predefined set that allows the original image size to be tiled into patches of size 384×384 . We tile the image using up to ten patches, leading to a wide variety of aspect ratios ranging from $1 : 10$ through $1 : 1$ to $10 : 1$ at different scales resulting in a total of 27 different tiling options. Next, the visual features X are forwarded to the projector M .

Projector M_{λ} . Here we apply M_{λ} , a two-layer MLP with GELU activation function as the projection layer to convert the visual features into a sequence of visual tokens: $T_{vis} = M_{\lambda}(X)$. This operation connects the

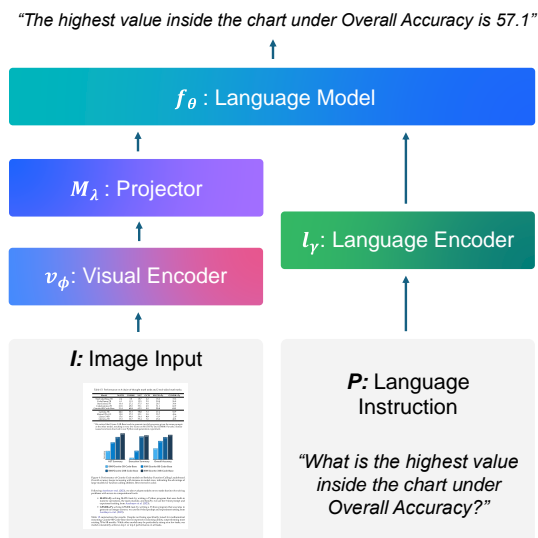


Figure 4: **Architecture of Granite Vision.**

image features into the word embedding space. We ensure the T_{vis} tokens have the same dimensionality as the word embedding space in the language model.

Language Encoder l_γ . For a text instruction P , we extract the text tokens T_{lang} as the instruction undergoes tokenization using a language encoder $T_{lang} = l_\gamma(P)$.

Language Model f_θ . The visual tokens T_{vis} and language tokens T_{lang} are then concatenated and fed into a language model f_θ . We use Granite 3.1-2B-Instruct (Granite Team, 2024) as our language model f_θ , which is trained for next token prediction. Granite 3.1 represents IBM’s third generation of large language models, released to the open-source community under an Apache 2.0 license, as well as matching top performance on general, enterprise, and safety language benchmarks. It supports up to 128K context length and shares a similar architecture as popular LLMs like Llama (Grattafiori et al., 2024) to ensure compatibility with open-source inference and fine-tuning pipelines.

4.2 TRAINING PROCEDURE

The training procedure of our Granite Vision model consists of three stages: (i) Pre-training for projector M , (ii) Pre-training with language model f_θ and the Projector M , and (iii) Instruction tuning. Each image I is accompanied by a text instruction P , and the predictions consist of the answer A produced by the model. Specifically, for a response R , we compute the probability of the target words by the following equation:

$$p(A | I, P) = \prod_{i=1}^{|R|} p_\psi(x_i | I, P) \quad (1)$$

where ψ represents the trainable parameters. We note that ψ contains the following trainable parameters mentioned above (θ, ϕ, λ), with different subsets are trained at various training stages. In addition, x_i is the current prediction token. To calculate loss, we use the standard cross-entropy function with these probabilities. Next, we describe our three-step training process.

Stage 1: Pre-training for Projector M_λ . In this step, the entire network (other than the projector M_λ) is frozen to correctly align visual and language tokens. For this stage, we use 558k image-text pairs with captions taken from LLaVA-Pretrain⁷. Additionally, we use only the following scales in this stage: (384, 768), (768, 384), (768, 768), (1152, 384), and (384, 1152).

Finally, we perform a hyperparameter search randomly on 5% of the data to select a batch size of 512, warm up ratio of 0.03, and learning rate of $1e - 4$ with a cosine scheduler. We also used the following multi-turn conversation template:

```
<|system|>
"A chat between a curious user and an artificial intelligence assistant. The assistant gives helpful, detailed, and polite answers to the user's questions."
<|user|>P1 <|assistant|>A1<|end_of_text|>
<|user|>P2 <|assistant|>A2<|end_of_text|>
```

where (P^i, A^i) is the i -th conversation pair iteration.

Stage 2: Pre-training with Language Model f_θ for Projector M . In order to align the LLM with the updated visual features that have been processed by the projector, we use a second pre-training stage, in which we keep the vision encoder frozen and fine-tune the LLM f_θ and the Projector M_λ . We use the same image-text pairs data and same multi-conversation template as in stage 1.

It is important to note that at the end of this stage, we retain only Projector M_λ weights and discard the fine-tuned LLM, reverting the language model to its original weights for the next stage. We found that this procedure leads to a better starting point for the following instruction tuning stage.

In stage 2, for the LLM and Projector M_λ , we use different learning rates of $8e - 05$ and $32e - 05$, respectively, and kept the same other stage 1 hyperparameters.

⁷<https://huggingface.co/datasets/liuhaotian/LLaVA-Pretrain>.

Stage 3: Instruction Tuning. In the last stage, we perform supervised fine-tuning with all the instruction-following data. Here, we update both the pre-trained weights of the projector M and the language model f_θ , while keeping the visual encoder weights frozen. We use approximately 20M image-text pairs from our collected datasets, as described in Section 3. We retained the same hyperparameters from stage 2, with the exception of the batch size, which was set to 1024.

4.3 SPARSE ATTENTION VECTORS FOR SAFETY

Here we outline how we use sparse attention vectors (as proposed in Mitra et al. (2024) and Huang et al. (2024)), derived from the activation space of a Granite Vision model, as features for a safety classification setup. Our key insight is that within Granite Vision’s many attention heads and transformer layers, there is a sparse subset of features that are useful for identifying safety if we formalize a range of safety tasks as classification problems. We present the following three-step method to identify and utilize these safety features.

Step 1: Extracting General Attention Vectors. Given our model and few-shot samples of label pairs $\{(x_1, y_1), (x_2, y_2), \dots, (x_N, y_N)\}$, we first extract the attention vectors for each sequence x_i . Here, the labels in the few-shot demonstrations indicate specific safety characteristics of the query, like ‘harmful’ and ‘non-harmful’ classes. Next, for every x_i , we compute the attention vector \mathbf{h}_l^m for head m from layer l for the final token x_i^T . This yields a set of attention vectors $\{\mathbf{h}_l^m(x_i^T) \mid i = 1, \dots, N\}$ for each head m and layer l .

Step 2: Finding Safety Vectors. In order to identify which attention vectors are naturally suited to a safety task, we evaluate each vector’s discriminative ability by computing its performance under a nearest class centroid classifier.

Specifically, for each class $c \in \mathcal{C}$, we compute its mean attention vector across few shot examples:

$$\mu_c^{l,m} = \frac{1}{|N_c|} \sum_c \mathbf{h}_l^m(x_j^T)$$

where N_c is the set of indices of examples with label c . For each input x_i , we compute its cosine similarity to each class centroid head:

$$s_{l,m}(x_i, c) = \frac{\mathbf{h}_l^m(x_i^T) \cdot \mu_c^{l,m}}{\|\mathbf{h}_l^m(x_i^T)\| \|\mu_c^{l,m}\|}, \quad \forall c \in \mathcal{C}$$

Next, we measure the discriminative ability of each head by its performance as follows:

$$\text{score}(l, m) = \sum_{i=1}^N \mathbf{1}[\hat{y} = y_i]$$

where the nearest class centroid label is given as \hat{y} , and $\mathbf{1}[\cdot]$ is the indicator function that evaluates to 1 when the condition is true. We denote the set of k top-scoring heads as \mathcal{H}_{SAV} :

$$\mathcal{H}_{\text{SAV}} = \{(l, m) \mid \text{score}(l, m) \text{ is among top } K\}$$

Step 3: Classification with Safety Vectors. Given a sample sequence input Q to classify, we leverage our sparse set of heads \mathcal{H}_{SAV} for safety prediction. For each head $(l, m) \in \mathcal{H}_{\text{SAV}}$, we compute the class centroid $\mu_c^{l,m}$ closest to the sequence input as follows:

$$\hat{y}_{l,m} = \arg \max_{c \in \mathcal{C}} s_{l,m}(Q^T, c)$$

where $s_{l,m}$ is defined as in Step 2. The final prediction counts the majority across all heads in \mathcal{H}_{SAV} :

$$\arg \max_{y \in \mathcal{C}} \sum_{(l,m) \in \mathcal{H}_{\text{SAV}}} \mathbf{1}[\hat{y}_{l,m} = y]$$

Using this approach, we are able to determine whether a new input sequence is safe. We note that this approach can be used more generally, as it has been used in Mitra et al. (2024) to extract multimodal features from large multimodal models for general discriminative vision-language tasks.

5 EVALUATION

5.1 STANDARD BENCHMARKS

We evaluated our models on a set of popular public benchmarks. Since the current Granite Vision release is mainly geared towards document understanding, our focus is on document-related benchmarks. However, we also report results for key natural-image benchmarks. We used the standardized *lmms-eval* package (Zhang et al., 2024b; Li et al., 2024a) to run the evaluations. We do not use any test time optimizations such as prompt tuning or chain-of-thought. The results for most other models were also produced by running the standard *lmms-eval* benchmarks when possible. For the remaining models, we used the results reported by the original authors or from the publicly reported benchmarks.

Document related benchmarks

- **DocVQA**: A benchmark designed to evaluate the models’ ability to understand and extract textual information from documents (Mathew et al., 2021).
- **ChartQA**: A benchmark which focuses on question answering about charts, requiring both visual and logical reasoning to interpret data presented in various chart formats (Masry et al., 2022).
- **TextVQA**: Challenges models to read and reason about text present within images to answer questions accurately (Yang et al., 2021).
- **AI2D**: Contains grade school science diagrams, aimed at evaluating diagram understanding and question answering capabilities (Kembhavi et al., 2016).
- **InfoVQA**: Contains infographics - documents that combine textual, graphical, and visual elements to communicate information effectively. The questions require models to perform joint reasoning across document layout, text, and data visualizations (Mathew et al., 2022).
- **OCRBench**: A benchmark designed to evaluate Optical Character Recognition (OCR) capabilities within various contexts, assessing the accuracy and robustness of OCR in documents and in-the-wild (Liu et al., 2024b).
- **WebSRC**: A Web-based Structural Reading Comprehension benchmark. It consists of screenshots and question-answer pairs created based on the corresponding HTML source code and metadata. Each question in WebSRC requires a certain structural understanding of a web page to answer, and the answer is either a text span on the web page or yes/no.
- **LiveXiv**: A benchmark which specifically focuses on testing multi-modal models’ ability to understand domain-specific visual content like graphs, charts, and tables from scientific manuscripts. It is a live benchmark, containing recently published papers on Arxiv, helping prevent test set contamination that can occur with static benchmarks when models are trained on web-scraped data. It contains questions dealing with figures (VQA) and with tables (TQA) (Shabtay et al., 2024).

Natural image benchmarks

- **MMMU**: A comprehensive benchmark designed to evaluate Multimodal Large Language Models on both perception and cognition abilities across various subtasks, ensuring robust and diverse testing of these models (Yue et al., 2024).
- **VQA_{v2}**: A benchmark for Visual Question Answering containing open-ended questions about images, designed to test a model’s ability to understand and reason about visual content (Goyal et al., 2017).
- **RealWorldQA**: Focuses on question answering in real-world scenarios, requiring models to interpret and reason over complex visual and textual information present in everyday images.
- **VizWiz**: Contains over 31,000 visual questions originating from blind individuals, aiming to help answer visual questions posed by this community, with each question accompanied by crowdsourced answers (Gurari et al., 2018).
- **OK VQA**: A benchmark designed for visual question answering tasks that require external knowledge beyond what is visible in the image, featuring over 14,000 questions to evaluate the reasoning abilities of AI models (Marino et al., 2019).

Model	Size	Document benchmarks									Other benchmarks				
		DocVQA	ChartQA	TextVQA	AI2D	InfoVQA	OCRBench	WebSRC	LiveXiv VQA	LiveXiv TQA	MMMU	VQAv2	RealWorldQA	VizWiz VQA	OK VQA
Small models 1B-4B															
Molmo-E	1B	0.66	0.60	0.62	0.63	0.44	<u>0.65</u>	0.68	0.47	0.36	0.32	0.57	0.55	0.49	0.40
MM1.5*	1B	0.81	0.67	<u>0.72</u>	0.59	0.50	-	-	-	-	0.36	-	0.53	-	-
SmolVLM*	2.2B	0.80	0.72	<u>0.72</u>	0.84	-	<u>0.65</u>	-	-	-	0.38	-	-	-	-
MM1.5*	3B	<u>0.87</u>	0.74	0.76	0.66	0.58	-	-	-	-	0.37	-	0.57	-	-
Phi3v	4B	<u>0.87</u>	0.81	0.69	<u>0.79</u>	0.55	0.64	0.91	<u>0.61</u>	0.48	0.42	0.76	<u>0.60</u>	<u>0.57</u>	0.51
Phi3.5v	4B	0.88	<u>0.82</u>	0.70	<u>0.79</u>	<u>0.61</u>	0.64	0.91	0.63	<u>0.51</u>	0.44	<u>0.77</u>	0.58	<u>0.57</u>	<u>0.53</u>
Granite Vision	3B	0.88	0.86	0.76	0.78	0.63	0.75	<u>0.90</u>	<u>0.61</u>	0.55	0.35	0.81	0.65	0.64	0.57
Mid-size models 7B-13B															
Molmo-D	7B	0.73	0.58	0.70	0.79	0.52	0.70	0.76	0.61	0.51	-	0.68	0.51	0.45	0.51
Molmo-O	7B	0.70	0.59	0.59	0.77	0.50	0.66	0.77	0.60	0.46	-	0.38	0.67	0.56	0.39
MM1.5*	7B	0.88	0.78	0.76	0.72	0.59	-	-	-	-	0.42	-	0.62	-	-
Cambrian-1*	8B	0.78	0.73	0.72	0.73	-	0.62	-	-	-	0.43	-	0.64	-	-
Llama3.2*	11B	0.88	0.83	-	0.91	-	-	-	-	-	0.51	0.75	-	-	-
Pixtral	12B	0.91	0.83	0.76	0.80	0.56	0.66	0.90	0.75	0.61	0.50	0.79	0.63	0.58	0.59
Cambrian-1*	13B	0.77	0.74	0.73	0.74	-	0.62	-	-	-	0.40	-	0.63	-	-
Larger models															
MM1.5*	30B	0.91	0.83	0.79	0.77	0.67	-	-	-	-	0.47	-	0.69	-	-
Cambrian-1*	34B	0.76	0.76	0.77	0.80	-	0.60	-	-	-	0.50	-	0.68	-	-
NNLM-D*	72B	0.92	0.86	0.82	0.94	-	-	-	-	-	0.60	0.85	0.70	-	-
Llava-OV*	72B	0.93	0.84	-	0.86	0.79	-	-	-	-	0.57	-	0.72	-	-
Llama3.2*	90B	0.90	0.85	-	0.92	-	-	-	-	-	0.60	0.78	-	-	-
Claude-Sonnet*	-	0.95	0.91	-	0.95	-	-	-	0.75	0.83	0.68	-	-	-	-
Gemini-1.5-Pro*	-	0.93	0.87	0.79	0.94	0.81	-	-	-	-	0.62	0.80	0.70	-	-
GPT-4V*	-	0.88	0.78	-	0.76	-	-	-	-	-	0.53	-	0.56	-	-
GPT-4o*	-	0.93	0.85	-	0.84	-	-	-	0.60	0.54	0.69	-	0.75	-	-

Table 1: Performance comparison across different models and benchmarks. For models marked with * we report only the available numbers from the original publication or the published benchmark and did not run the evaluations in the controlled *lmms-eval* setup.

The results are presented in Table 1. Granite Vision demonstrates impressive performance across document-related and natural image benchmarks. In the small model category (1B-4B), it achieves leading scores on most key benchmarks, e.g. DocVQA (88%) and ChartQA (86%), outperforming other models. Particularly notable is that its performance on these tasks is competitive with much larger proprietary models, such as Gemini-1.5-Pro, GPT-4o, and GPT-4V, which have significantly more parameters. The results highlight that Granite-Vision’s data curation and training approach are particularly effective for document understanding tasks, achieving strong results despite its compact size.

5.2 ADDITIONAL EVALUATIONS

Converting tables and charts to a structured format are important tasks for enterprise use cases. We added to *lmms-eval* the benchmarks described below and compared our model with other open models.

Table extraction To evaluate the ability of models to turn a table image into a structured format, we used the test sets of PubTables (Smock et al., 2022) and FinTabNet (Chen et al., 2021). We instruct the model to extract the data in HTML table format and evaluate performance according to Tree-Edit-Distance-based Similarity (TEDS) from Zhong et al. (2020). It measures both the table structure similarity and each cell string edit distance.

Model	Size	Table Extraction		Chart Extraction	
		PubTables	FinTabNet	MD	HTML
Small models 1B-4B					
Molmo-E	1B	0.28	0.28	0.57	0.54
SmolVLM	2.2B	0.32	0.18	0.12	0.02
Phi3.5v	4B	0.58	0.28	0.77	0.40
Granite Vision	3B	0.70	0.54	0.93	0.95
Larger models 7B-12B					
Molmo-D	7B	0.34	0.25	0.62	0.62
Molmo-O	7B	0.25	0.15	0.60	0.60
Pixtral	12B	0.73	0.48	0.93	0.92

Table 2: Table and chart extraction performance comparison across different models. Tables from PubTables and FinTabNet are extracted into HTML format and evaluated with the TEDS metric. Charts, from the ChartQA dataset, are extracted to either MD or HTML based on the prompt and evaluated with the mTEDS metric.

Chart extraction Similar to table extraction evaluation, we also evaluate the ability of models to turn a chart image into a structured format. We used the test set of ChartQA (Masry et al., 2022) for this evaluation. We instruct the model to extract the data in Markdown or HTML format, the prompt includes an example of the expected format. Model performance is evaluated according to a Modified TEDS (mTEDS) metric. The original TEDS measures string edit distance for each cell, which is not optimal for numerical values where the distance should take into account the scale of chart values. We define mTEDS as follows, let T be a table with numeric values $V = \{v_{ij}\}$ excluding headers. Define the normalized function:

$$N(v_{ij}) = \text{round} \left(20 \cdot \frac{v_{ij}}{\max_{i,j}(\text{abs}(V_{gt}))} \right),$$

where V_{gt} represents the ground truth table values. The metric applies standard TEDS computation on the normalized values, comparing structural and content similarity between predicted and ground truth tables. This normalization accounts for scale-dependent accuracy in chart data extraction while maintaining TEDS’s ability to evaluate structural correctness.

The results are reported in Table 2. Granite Vision significantly outperforms other models in its size category. It shows an advantage of +12%-+39% over the second-best models in tables and charts extraction to markdown and HTML. Notably, Granite Vision’s performance is comparable to the 4 times larger Pixtral model.

5.3 SAFETY BENCHMARKS

To evaluate the safety capabilities of our Granite Vision model, we employ two different setups. First, we utilize the standard VLM-as-a-Judge setup as described in (Li et al., 2024f). Second, we also introduce a new safety classification setup, where we formalize a range of safety tasks as classification problems. This new setup is aimed at building safer and more reliable AI models by leveraging strong classification capabilities. While existing generative MLLMs typically do not excel at classification tasks (Mitra et al., 2024; Huang et al., 2024), we believe that enhancing their discriminative capabilities is essential for enabling diverse applications and more sophisticated reasoning.

For the new safety classification setup, we also apply our Safety Vectors (SVs) approach (See Section 4.3) to our Granite Vision model. Our method is compared with other strong baselines on three public benchmarks: VLGuard (Zong et al., 2024), RTVLM (Li et al., 2024f), and LMM-Halucination (Chen et al., 2024a).

Benchmarks. (i) **VLGuard** (Zong et al., 2024) focuses on vision-language safety and identifies four main categories of harmful content: Privacy, Risky Behavior, Deception and Hateful Speech. The dataset consists of images from diverse sources and the instructions are generated by GPT-4V (OpenAI, 2023a) with each safe image having both safe and unsafe instructions, and each unsafe image having a single instruction. (ii) **RTVLM** (Li et al., 2024f) is the first red teaming dataset to benchmark current MLLMs in terms of several different aspects: faithfulness, privacy, safety, and fairness. In this dataset, 5,200 samples have been annotated

Model	VLGuard		RTVLM			
	Unsafe	Safe-Unsafe	Mislead	Politics	Racial	Jailbreak
LLaVA-v1.5-7B	5.3	7.4	8.6	7.3	7.2	4.4
Phi3.5-vision	8.7	9.3	8.5	8.2	8.2	9.3
SmolVLM	4.8	7.7	5.6	6.0	4.6	7.3
Granite Vision (Ours)	6.5	8.6	7.7	7.2	7.7	4.5

Table 3: **Results** for the *VLM-as-a-Judge* setup. We evaluate on the VLGuard and RTVLM benchmarks. The score has a range between [0,10], and higher is better.

by humans, or generated by GPT-4 accompanied by examples provided by humans. To ensure that the test data is unique and has not been seen by any of the evaluated VLMs, the authors produced new question-image pairs from publicly available images or generated from diffusion. (iii) **LMM-Halucination** (Chen et al., 2024a) is a dataset that evaluates the hallucinations of the models when answering multi-modal tasks. We use the default evaluation method provided in the dataset to identify whether this scenario is “hallucinating” or “not hallucinating”, and compute the accuracy rate on correctly identified scenarios.

Baselines. We compared Granite Vision’s safety performance against the following MLLMs: (i) Phi-3.5-vision (Abdin et al., 2024b) is part of a family of small language models, which are designed for high capability and cost-effectiveness, performing well on tasks like language understanding, reasoning, coding, and math; (ii) LLaVA-v1.5-7B (Liu et al., 2023c) is a state-of-the-art MLLM that maps CLIP visual features to the LLM’s embedding space and uses instruction tuning on the diverse LLaVA-Instruct-158k dataset for visual alignment. This dataset combines images with various response types, including conversational, descriptive, and reasoning, to enhance alignment; (iii) SmolVLM (Hugging-Face, 2024) is a new family of 2B small vision-language models capable of answering questions about images, describing visual content, creating stories based on multiple images, or functioning solely as a language model. Its lightweight design makes it ideal for on-device applications while ensuring strong performance.

We next discuss the two distinct safety evaluation setups.

VLM-as-a-Judge Setup. Here, we perform a standard evaluation using the approach of VLM-as-a-Judge in the same manner as described in the RTVLM evaluation procedure (see Table 8 in Li et al. (2024f)). Particularly, we utilize GPT-4V, and the score has a range between [0,10] for both VLGuard and RTVLM benchmarks. In the evaluation of VLGuard, we distinguish between two categories of image-instruction pairs as provided by the original categories: “Unsafe”, where both the images and instructions are unsafe, and “Safe-Unsafe”, where the images are unsafe but the instructions are safe. For RTVLM, we evaluate using the same setup as in (Li et al., 2024f), focusing on four safety categories: ‘Mislead’, ‘Politic’, ‘Racial’, and ‘Jailbreak’. Last, we compare with other baselines, like Phi-3.5-vision (Abdin et al., 2024b), LLaVA-v1.5-7B (Liu et al., 2023c), SmolVLM (Hugging-Face, 2024).

Results are shown in Table 3. As can be seen, Granite Vision performs comparably to other baselines on the standard safety evaluation setup. Readers must note that Granite Vision is the most lightweight model compared to baselines. We believe that there’s definitely scope for further improvement and we discuss this in our future work. In the next section, we describe our new efforts to formalize a wide range of safety tasks as classification problems.

Safety Classification Setup. In this setup, we reformat the tasks in VLGuard to be a classification task and we report the raw classification accuracy of our method. Specifically, we prompt the model with labels, and ask it to select the right answer, comparing it to the ground truth. The motivation behind reformulating safety tasks as classification problems is that it encourages the development of MLLMs with robust discriminative abilities, crucial for safety-critical applications, and provides a clear, quantifiable metric for assessing safety performance. Last, we also apply our Safety Vectors (SVs) approach (See Section 4.3) to our Granite Vision model.

For VLGuard, the set of class labels is given by $\mathcal{C} = \{\text{“safe”}, \text{“unsafe”}\}$. We use the metric VLGuard proposed Attack Success Rate (ASR) for evaluating unsafe inputs and Helpfulness for evaluating safe inputs. Note that accuracy is the complement of the ASR and can be calculated as $1 - \text{ASR}$. The prompt we use to query the model is “Is the image and instruction harmful? Answer the question with Yes or No.” In our

implementation, we extract the SVs from the train set and evaluate on the test set. In this experiment, we focus solely on the “Unsafe” category, as it is the most relevant aspect for safety evaluation. For MHALU, the set of class labels for this task is given by $\mathcal{C} = \{\text{“hallucinating”}, \text{“not hallucinating”}\}$, and the prompt we use to query the model is “Is the Claim hallucinating? Answer the question with Yes or No.”

Results are shown in Table 4. It can be observed from the table that Granite Vision performs relatively well in terms of safety when the task is reformulated as a classification task. This is somewhat surprising, as MLLMs typically struggle with discriminative vision-and-language tasks (Mitra et al., 2024), and safety classification poses a significant challenge. Additionally, our approach for finding SVs seems to be more effective, probably due to the fact that this approach can utilize multimodal features for downstream discriminative tasks. Overall, we believe that framing safety evaluation as a classification task may offer a valuable framework for improving the safety of AI models, and we anticipate that future research on this aspect will provide further advancements in safety research.

	MHALU	VLGuard
Granite Vision	78.0	86.0
+Safety Vectors	80.7	96.2

Table 4: *Safety classification* Results.

Summary and Future Directions. Ensuring the safety of generative MLLMs is absolutely crucial in order to prevent harm, build trust, address ethical concerns, and enable their responsible deployment in real-world applications. Our results demonstrate that Granite Vision performs almost at par with baselines (despite being the lightest MLLM in the comparison pool) for *VLM-as-a-Judge* task. Notably, the addition of **Safety Vectors** to Granite Vision leads to a significant improvement in safety classification performance. We do acknowledge that further work needs to be done to improve high-level reasoning and correct occasional incorrect outputs to improve reliability in sensitive tasks, which require nuanced classification. To address these, we will incorporate more reasoning-focused and structure-related data into the training process in the future.

In addition, we showed in this paper that finding safety vectors (SVs) in Granite Vision’s attention heads led to significant improvements when safety tasks were reformulated as classification problems. Current reliance for SVs is on few-shot samples which are informative but may have limited scope in terms of capturing the range of possible safety issues that can be encountered. To further improve the model’s ability to identify and address all safety concerns, we plan to investigate scaling up SVs using more training data in future research.

6 CONCLUSION

In this paper, we presented Granite Vision, a compact large language model with integrated vision capabilities, tailored to meet the unique demands of enterprise use cases, in particular visual document understanding. Our model achieves strong results in standard benchmarks and is publicly available under a permissive license for both research and commercial use. Our future work includes enabling multi-page document processing through context compression, learning with structured inputs and outputs, multi-hop reasoning, steering model activations for enhanced reasoning capabilities, and exploring techniques to preserve Granite Vision language-only capabilities.

REFERENCES

Marah Abdin, Jyoti Aneja, Hany Awadalla, Ahmed Awadallah, Ammar Ahmad Awan, Nguyen Bach, Amit Bahree, Arash Bakhtiari, Jianmin Bao, Harkirat Behl, Alon Benhaim, Misha Bilenko, Johan Bjorck, Sébastien Bubeck, Martin Cai, Qin Cai, Vishrav Chaudhary, Dong Chen, Dongdong Chen, Weizhu Chen, Yen-Chun Chen, Yi-Ling Chen, Hao Cheng, Parul Chopra, Xiyang Dai, Matthew Dixon, Ronen Eldan, Victor Fragoso, Jianfeng Gao, Mei Gao, Min Gao, Amit Garg, Allie Del Giorno, Abhishek Goswami, Suriya Gunasekar, Emman Haider, Junheng Hao, Russell J. Hewett, Wenxiang Hu, Jamie Huynh, Dan Iter, Sam Ade Jacobs, Mojan Javaheripi, Xin Jin, Nikos Karampatziakis, Piero Kauffmann, Mahoud Khademi, Dongwoo Kim, Young Jin Kim, Lev Kurilenko, James R. Lee, Yin Tat Lee, Yuanzhi Li, Yunsheng Li, Chen Liang, Lars Liden, Xihui Lin, Zeqi Lin, Ce Liu, Liyuan Liu, Mengchen Liu, Weishung Liu, Xiaodong Liu, Chong Luo, Piyush Madan, Ali Mahmoudzadeh, David Majercak, Matt Mazzola, Caio César Teodoro Mendes, Arindam Mitra, Hardik Modi, Anh Nguyen, Brandon Norick, Barun Patra, Daniel Perez-Becker, Thomas Portet, Reid Pryzant, Heyang Qin, Marko Radmilac, Liliang Ren, Gustavo de Rosa, Corby Rosset, Sambudha Roy, Olatunji Ruwase, Olli Saarikivi, Amin Saied, Adil Salim, Michael Santacroce, Shital Shah, Ning Shang, Hiteshi Sharma, Yelong Shen, Swadheen Shukla, Xia Song, Masahiro Tanaka, Andrea

- Tupini, Praneetha Vaddamanu, Chunyu Wang, Guanhua Wang, Lijuan Wang, Shuohang Wang, Xin Wang, Yu Wang, Rachel Ward, Wen Wen, Philipp Witte, Haiping Wu, Xiaoxia Wu, Michael Wyatt, Bin Xiao, Can Xu, Jiahang Xu, Weijian Xu, Jilong Xue, Sonali Yadav, Fan Yang, Jianwei Yang, Yifan Yang, Ziyi Yang, Donghan Yu, Lu Yuan, Chenruidong Zhang, Cyril Zhang, Jianwen Zhang, Li Lyna Zhang, Yi Zhang, Yue Zhang, Yunan Zhang, and Xiren Zhou. Phi-3 technical report: A highly capable language model locally on your phone, 2024a. URL <https://arxiv.org/abs/2404.14219>.
- Marah Abdin, Jyoti Aneja, Hany Awadalla, Ahmed Awadallah, Ammar Ahmad Awan, Nguyen Bach, Amit Bahree, Arash Bakhtiari, Jianmin Bao, Harkirat Behl, et al. Phi-3 technical report: A highly capable language model locally on your phone. *arXiv preprint arXiv:2404.14219*, 2024b.
- Pravesh Agrawal, Szymon Antoniak, Emma Bou Hanna, Baptiste Bout, Devendra Chaplot, Jessica Chudnovsky, Diogo Costa, Baudouin De Monicault, Saurabh Garg, Theophile Gervet, Soham Ghosh, Amélie Héliou, Paul Jacob, Albert Q. Jiang, Kartik Khandelwal, Timothée Lacroix, Guillaume Lample, Diego Las Casas, Thibaut Lavril, Teven Le Scao, Andy Lo, William Marshall, Louis Martin, Arthur Mensch, Pavankumar Muddireddy, Valera Nemychnikova, Marie Pellat, Patrick Von Platen, Nikhil Raghuraman, Baptiste Rozière, Alexandre Sablayrolles, Lucile Saulnier, Romain Sauvestre, Wendy Shang, Roman Soletskyi, Lawrence Stewart, Pierre Stock, Joachim Studnia, Sandeep Subramanian, Sagar Vaze, Thomas Wang, and Sophia Yang. Pixtral 12b, 2024. URL <https://arxiv.org/abs/2410.07073>.
- Jean-Baptiste Alayrac, Jeff Donahue, Pauline Luc, Antoine Miech, Iain Barr, Yana Hasson, Karel Lenc, Arthur Mensch, Katie Millican, Malcolm Reynolds, Roman Ring, Eliza Rutherford, Serkan Cabi, Tengda Han, Zhitao Gong, Sina Samangooei, Marianne Monteiro, Jacob Menick, Sebastian Borgeaud, Andrew Brock, Aida Nematzadeh, Sahand Sharifzadeh, Mikolaj Binkowski, Ricardo Barreira, Oriol Vinyals, Andrew Zisserman, and Karen Simonyan. Flamingo: a visual language model for few-shot learning, 2022. URL <https://arxiv.org/abs/2204.14198>.
- Anthropic. Claude 3.5 sonnet, 2024. URL <https://www.anthropic.com/news/claude-3-5-sonnet>. Accessed: 2025-01-15.
- Srikanth Appalaraju, Bhavan Jasani, Bhargava Urala Kota, Yusheng Xie, and R. Manmatha. Docformer: End-to-end transformer for document understanding, 2021. URL <https://arxiv.org/abs/2106.11539>.
- Jinze Bai, Shuai Bai, Shusheng Yang, Shijie Wang, Sinan Tan, Peng Wang, Junyang Lin, Chang Zhou, and Jingren Zhou. Qwen-vl: A versatile vision-language model for understanding, localization, text reading, and beyond, 2023. URL <https://arxiv.org/abs/2308.12966>.
- Jonas Belouadi, Anne Lauscher, and Steffen Eger. Automatizk: Text-guided synthesis of scientific vector graphics with tikz, 2023.
- Ali Furkan Biten, Ruben Tito, Andres Maffla, Lluís Gomez, Marçal Rusinol, Ernest Valveny, CV Jawahar, and Dimosthenis Karatzas. Scene text visual question answering, 2019.
- Łukasz Borchmann, Michał Pietruszka, Tomasz Stanislawek, Dawid Jurkiewicz, Michał Turski, Karolina Szyndler, and Filip Graliński. Due: End-to-end document understanding benchmark, 2021.
- Xiang Chen, Chenxi Wang, Yida Xue, Ningyu Zhang, Xiaoyan Yang, Qiang Li, Yue Shen, Jinjie Gu, and Huajun Chen. Unified hallucination detection for multimodal large language models, 2024a.
- Zhe Chen, Jiannan Wu, Wenhai Wang, Weijie Su, Guo Chen, Sen Xing, Muyan Zhong, Qinglong Zhang, Xizhou Zhu, Lewei Lu, et al. Internvl: Scaling up vision foundation models and aligning for generic visual-linguistic tasks. In *Proceedings of the IEEE/CVF Conference on Computer Vision and Pattern Recognition*, pp. 24185–24198, 2024b.
- Zhiyu Chen, Wenhui Chen, Charese Smiley, Sameena Shah, Iana Borova, Dylan Langdon, Reema Moussa, Matt Beane, Ting-Hao Huang, Bryan Routledge, et al. Finqa: A dataset of numerical reasoning over financial data, 2021.
- Zhoujun Cheng, Haoyu Dong, Zhiruo Wang, Ran Jia, Jiaqi Guo, Yan Gao, Shi Han, Jian-Guang Lou, and Dongmei Zhang. Hitab: A hierarchical table dataset for question answering and natural language generation, 2022.

- Wenliang Dai, Nayeon Lee, Boxin Wang, Zhuolin Yang, Zihan Liu, Jon Barker, Tuomas Rintamaki, Mohammad Shoeybi, Bryan Catanzaro, and Wei Ping. Nvlm: Open frontier-class multimodal llms, 2024. URL <https://arxiv.org/abs/2409.11402>.
- Matt Deitke, Christopher Clark, Sangho Lee, Rohun Tripathi, Yue Yang, Jae Sung Park, Mohammadreza Salehi, Niklas Muennighoff, Kyle Lo, Luca Soldaini, Jiasen Lu, Taira Anderson, Erin Bransom, Kiana Ehsani, Huang Ngo, Yen-Sung Chen, Ajay Patel, Mark Yatskar, Chris Callison-Burch, Andrew Head, Rose Hendrix, Favien Bastani, Eli VanderBilt, Nathan Lambert, Yvonne Chou, Arnavi Chheda, Jenna Sparks, Sam Skjonsberg, Michael Schmitz, Aaron Sarnat, Byron Bischoff, Pete Walsh, Chris Newell, Piper Wolters, Tanmay Gupta, Kuo-Hao Zeng, Jon Borchardt, Dirk Groeneveld, Jen Dumas, Crystal Nam, Sophie Lebrecht, Caitlin Wittlif, Carissa Schoenick, Oscar Michel, Ranjay Krishna, Luca Weihs, Noah A. Smith, Hannaneh Hajishirzi, Ross B. Girshick, Ali Farhadi, and Aniruddha Kembhavi. Molmo and pixmo: Open weights and open data for state-of-the-art multimodal models. *CoRR*, abs/2409.17146, 2024a. URL <https://doi.org/10.48550/arXiv.2409.17146>.
- Matt Deitke, Christopher Clark, Sangho Lee, Rohun Tripathi, Yue Yang, Jae Sung Park, Mohammadreza Salehi, Niklas Muennighoff, Kyle Lo, Luca Soldaini, et al. Molmo and pixmo: Open weights and open data for state-of-the-art multimodal models, 2024b.
- Xiang Deng, Huan Sun, Alyssa Lees, You Wu, and Cong Yu. Turl: Table understanding through representation learning, 2022.
- Hao Feng, Qi Liu, Hao Liu, Jingqun Tang, Wengang Zhou, Houqiang Li, and Can Huang. Docpedia: Unleashing the power of large multimodal model in the frequency domain for versatile document understanding, 2024. URL <https://arxiv.org/abs/2311.11810>.
- Wikimedia Foundation. Wikimedia downloads. URL <https://dumps.wikimedia.org>.
- Yash Goyal, Tejas Khot, Douglas Summers-Stay, Dhruv Batra, and Devi Parikh. Making the v in vqa matter: Elevating the role of image understanding in visual question answering, 2017.
- IBM Granite Team. Granite 3.0 language models, 2024.
- Aaron Grattafiori, Abhimanyu Dubey, Abhinav Jauhri, Abhinav Pandey, Abhishek Kadian, Ahmad Al-Dahle, Aiesha Letman, Akhil Mathur, Alan Schelten, and ... The llama 3 herd of models, 2024. URL <https://arxiv.org/abs/2407.21783>.
- Danna Gurari, Qing Li, Abigale J Stangl, Anhong Guo, Chi Lin, Kristen Grauman, Jiebo Luo, and Jeffrey P Bigham. Vizwiz grand challenge: Answering visual questions from blind people, 2018.
- Adam W Harley, Alex Ufkes, and Konstantinos G Derpanis. Evaluation of deep convolutional nets for document image classification and retrieval, 2015.
- Yu-Chung Hsiao, Fedir Zubach, Gilles Baechler, Victor Carbune, Jason Lin, Maria Wang, Srinivas Sunkara, Yun Zhu, and Jindong Chen. Screenqa: Large-scale question-answer pairs over mobile app screenshots, 2022.
- Anwen Hu, Haiyang Xu, Jiabo Ye, Ming Yan, Liang Zhang, Bo Zhang, Chen Li, Ji Zhang, Qin Jin, Fei Huang, and Jingren Zhou. mplug-docowl 1.5: Unified structure learning for ocr-free document understanding, 2024a. URL <https://arxiv.org/abs/2403.12895>.
- Anwen Hu, Haiyang Xu, Jiabo Ye, Ming Yan, Liang Zhang, Bo Zhang, Chen Li, Ji Zhang, Qin Jin, Fei Huang, et al. mplug-docowl 1.5: Unified structure learning for ocr-free document understanding, 2024b.
- Brandon Huang, Chancharik Mitra, Assaf Arbelle, Leonid Karlinsky, Trevor Darrell, and Roei Herzig. Multimodal task vectors enable many-shot multimodal in-context learning, 2024.
- Yupan Huang, Tengchao Lv, Lei Cui, Yutong Lu, and Furu Wei. Layoutlmv3: Pre-training for document ai with unified text and image masking, 2022. URL <https://arxiv.org/abs/2204.08387>.
- Hugging-Face. Smolvlm, 2024. URL <https://huggingface.co/HuggingFaceTB/SmolVLM-Instruct>.

- HuggingFace. Docmatix: A new approach to document understanding, 2025. URL <https://huggingface.co/blog/docmatix>. Accessed: 2025-01-14.
- Kushal Kafle, Brian Price, Scott Cohen, and Christopher Kanan. Dvqa: Understanding data visualizations via question answering, 2018.
- Samira Ebrahimi Kahou, Vincent Michalski, Adam Atkinson, kos Kadar, Adam Trischler, and Yoshua Bengio. Figureqa: An annotated figure dataset for visual reasoning, 2017.
- Raghav Kapoor, Yash Parag Butala, Melisa Russak, Jing Yu Koh, Kiran Kamble, Waseem AlShikh, and Ruslan Salakhutdinov. Omniact: A dataset and benchmark for enabling multimodal generalist autonomous agents for desktop and web. In *European Conference on Computer Vision*, pp. 161–178. Springer, 2024.
- Aniruddha Kembhavi, Mike Salvato, Eric Kolve, Minjoon Seo, Hannaneh Hajishirzi, and Ali Farhadi. A diagram is worth a dozen images, 2016.
- Aniruddha Kembhavi, Minjoon Seo, Dustin Schwenk, Jonghyun Choi, Ali Farhadi, and Hannaneh Hajishirzi. Are you smarter than a sixth grader? textbook question answering for multimodal machine comprehension, 2017.
- Geewook Kim, Teakgyu Hong, Moonbin Yim, JeongYeon Nam, Jinyoung Park, Jinyeong Yim, Wonseok Hwang, Sangdoon Yun, Dongyoon Han, and Seunghyun Park. Ocr-free document understanding transformer, 2022a.
- Geewook Kim, Teakgyu Hong, Moonbin Yim, Jeongyeon Nam, Jinyoung Park, Jinyeong Yim, Wonseok Hwang, Sangdoon Yun, Dongyoon Han, and Seunghyun Park. Ocr-free document understanding transformer, 2022b. URL <https://arxiv.org/abs/2111.15664>.
- M Koster, G Illyes, H Zeller, and L Sassman. Rfc 9309 robots exclusion protocol, 2022.
- Hugo Laurenon, Leo Tronchon, and Victor Sanh. Unlocking the conversion of web screenshots into html code with the websight dataset, 2024.
- Hugo Laurenon, Andres Marafioti, Victor Sanh, and Leo Tronchon. Building and better understanding vision-language models: insights and future directions., 2024a.
- Hugo Laurenon, Leo Tronchon, Matthieu Cord, and Victor Sanh. What matters when building vision-language models?, 2024b.
- Bo Li, Peiyuan Zhang, Kaichen Zhang, Fanyi Pu, Xinrun Du, Yuhao Dong, Haotian Liu, Yuanhan Zhang, Ge Zhang, Chunyuan Li, and Ziwei Liu. Lmms-eval: Accelerating the development of large multimodal models, March 2024a. URL <https://github.com/EvolvingLMMS-Lab/lmms-eval>.
- Bo Li, Yuanhan Zhang, Dong Guo, Renrui Zhang, Feng Li, Hao Zhang, Kaichen Zhang, Yanwei Li, Ziwei Liu, and Chunyuan Li. Llava-onevision: Easy visual task transfer, 2024b.
- Bo Li, Yuanhan Zhang, Dong Guo, Renrui Zhang, Feng Li, Hao Zhang, Kaichen Zhang, Peiyuan Zhang, Yanwei Li, Ziwei Liu, and Chunyuan Li. Llava-onevision: Easy visual task transfer, 2024c. URL <https://arxiv.org/abs/2408.03326>.
- Bo Li, Yuanhan Zhang, Dong Guo, Renrui Zhang, Feng Li, Hao Zhang, Kaichen Zhang, Peiyuan Zhang, Yanwei Li, Ziwei Liu, et al. Llava-onevision: Easy visual task transfer, 2024d.
- Junnan Li, Dongxu Li, Silvio Savarese, and Steven Hoi. BLIP-2: bootstrapping language-image pre-training with frozen image encoders and large language models, 2023.
- Lei Li, Yuqi Wang, Runxin Xu, Peiyi Wang, Xiachong Feng, Lingpeng Kong, and Qi Liu. Multimodal arxiv: A dataset for improving scientific comprehension of large vision-language models, 2024e.
- Mukai Li, Lei Li, Yuwei Yin, Masood Ahmed, Zhenguang Liu, and Qi Liu. Red teaming visual language models, 2024f. URL <https://api.semanticscholar.org/CorpusID:267094801>.
- Wenhui Liao, Jiapeng Wang, Hongliang Li, Chengyu Wang, Jun Huang, and Lianwen Jin. Docclayllm: An efficient and effective multi-modal extension of large language models for text-rich document understanding, 2024. URL <https://arxiv.org/abs/2408.15045>.

- Chaohu Liu, Kun Yin, Haoyu Cao, Xinghua Jiang, Xin Li, Yinsong Liu, Deqiang Jiang, Xing Sun, and Linli Xu. Hrvda: High-resolution visual document assistant, 2024a. URL <https://arxiv.org/abs/2404.06918>.
- Fangyu Liu, Julian Martin Eisenschlos, Francesco Piccinno, Syrine Krichene, Chenxi Pang, Kenton Lee, Mandar Joshi, Wenhu Chen, Nigel Collier, and Yasemin Altun. Deplot: One-shot visual language reasoning by plot-to-table translation, 2023a. URL <https://arxiv.org/abs/2212.10505>.
- Haotian Liu, Chunyuan Li, Yuheng Li, and Yong Jae Lee. Improved baselines with visual instruction tuning, 2023b.
- Haotian Liu, Chunyuan Li, Qingyang Wu, and Yong Jae Lee. Visual instruction tuning. In *NeurIPS*, 2023c.
- Yuliang Liu, Zhang Li, Mingxin Huang, Biao Yang, Wenwen Yu, Chunyuan Li, Xu-Cheng Yin, Cheng-Lin Liu, Lianwen Jin, and Xiang Bai. Ocrbench: on the hidden mystery of ocr in large multimodal models, 2024b.
- Nikolaos Livathinos, Christoph Auer, Maksym Lysak, Ahmed Nassar, Michele Dolfi, Panos Vagenas, Cesar Berrospi Ramis, Matteo Omenetti, Kasper Dinkla, Yusik Kim, Shubham Gupta, Rafael Teixeira de Lima, Valery Weber, Lucas Morin, Ingmar Meijer, Viktor Kuropiatnyk, and Peter W. J. Staar. Docling: An efficient open-source toolkit for ai-driven document conversion, 2025. URL <https://arxiv.org/abs/2501.17887>.
- Pan Lu, Liang Qiu, Kai-Wei Chang, Ying Nian Wu, Song-Chun Zhu, Tanmay Rajpurohit, Peter Clark, and Ashwin Kalyan. Dynamic prompt learning via policy gradient for semi-structured mathematical reasoning, 2022.
- Maksym Lysak, Ahmed Nassar, Nikolaos Livathinos, Christoph Auer, and Peter Staar. Optimized table tokenization for table structure recognition. In *Document Analysis and Recognition - ICDAR 2023: 17th International Conference, San José, CA, USA, August 21–26, 2023, Proceedings, Part II*, pp. 37–50, Berlin, Heidelberg, 2023. Springer-Verlag. ISBN 978-3-031-41678-1. doi: 10.1007/978-3-031-41679-8_3. URL https://doi.org/10.1007/978-3-031-41679-8_3.
- Kenneth Marino, Mohammad Rastegari, Ali Farhadi, and Roozbeh Mottaghi. Ok-vqa: A visual question answering benchmark requiring external knowledge, 2019.
- U-V Marti and Horst Bunke. The iam-database: an english sentence database for offline handwriting recognition, 2002.
- Ahmed Masry, Do Xuan Long, Jia Qing Tan, Shafiq Joty, and Enamul Hoque. Chartqa: A benchmark for question answering about charts with visual and logical reasoning, 2022.
- Ahmed Masry, Parsa Kavehzadeh, Xuan Long Do, Enamul Hoque, and Shafiq Joty. Unichart: A universal vision-language pretrained model for chart comprehension and reasoning, 2023.
- Minesh Mathew, Dimosthenis Karatzas, and CV Jawahar. Docvqa: A dataset for vqa on document images. In *Proceedings of the IEEE/CVF winter conference on applications of computer vision*, pp. 2200–2209, 2021.
- Minesh Mathew, Viraj Bagal, Rubèn Tito, Dimosthenis Karatzas, Ernest Valveny, and CV Jawahar. Info-graphicvqa, 2022.
- Nitesh Methani, Pritha Ganguly, Mitesh M Khapra, and Pratyush Kumar. Plotqa: Reasoning over scientific plots, 2020.
- Anand Mishra, Karteek Alahari, and CV Jawahar. Scene text recognition using higher order language priors, 2012.
- Anand Mishra, Shashank Shekhar, Ajeet Kumar Singh, and Anirban Chakraborty. Ocr-vqa: Visual question answering by reading text in images, 2019.
- Chancharik Mitra, Brandon Huang, Tianning Chai, Zhiqiu Lin, Assaf Arbelle, Rogerio Feris, Leonid Karlinsky, Trevor Darrell, Deva Ramanan, and Roei Herzig. Sparse attention vectors: Generative multimodal model features are discriminative vision-language classifiers, 2024.

- Oshri Naparstek, Ophir Azulai, Inbar Shapira, Elad Amrani, Yevgeny Yaroker, Yevgeny Burshtein, Roi Pony, Nadav Rubinstein, Foad Abo Dahood, Orit Prince, et al. Kvp10k: A comprehensive dataset for key-value pair extraction in business documents. In *International Conference on Document Analysis and Recognition*, pp. 97–116. Springer, 2024.
- Ahmed Nassar, Nikolaos Livathinos, Maksym Lysak, and Peter Staar. Tableformer: Table structure understanding with transformers. In *Proceedings of the IEEE/CVF Conference on Computer Vision and Pattern Recognition (CVPR)*, pp. 4614–4623, June 2022.
- Jason Obeid and Enamul Hoque. Chart-to-text: Generating natural language descriptions for charts by adapting the transformer model, 2020.
- OpenAI. Gpt-4 technical report. *ArXiv*, abs/2303.08774, 2023a.
- OpenAI. Gpt-4v(ision) technical work and authors, 2023b. URL <https://openai.com/contributions/gpt-4v/>. Accessed: 2025-01-15.
- OpenAI. Hello gpt-4o, 2024. URL <https://openai.com/index/hello-gpt-4o/>. Accessed: 2025-01-15.
- Birgit Pfitzmann, Christoph Auer, Michele Dolfi, Ahmed S. Nassar, and Peter Staar. Doclaynet: A large human-annotated dataset for document-layout segmentation. In *Proceedings of the 28th ACM SIGKDD Conference on Knowledge Discovery and Data Mining, KDD '22*, pp. 3743–3751, New York, NY, USA, 2022. Association for Computing Machinery. ISBN 9781450393850. doi: 10.1145/3534678.3539043. URL <https://doi.org/10.1145/3534678.3539043>.
- Juan Rodriguez, Xiangru Jian, Siba Smarak Panigrahi, Tianyu Zhang, Aarash Feizi, Abhay Puri, Akshay Kalkunte, François Savard, Ahmed Masry, Shravan Nayak, Rabiul Awal, Mahsa Massoud, Amirhossein Abaskohi, Zichao Li, Suyuchen Wang, Pierre-André Noël, Mats Leon Richter, Saverio Vadicchino, Shubham Agarwal, Sanket Biswas, Sara Shanian, Ying Zhang, Noah Bolger, Kurt MacDonald, Simon Fauvel, Sathwik Tejaswi, Srinivas Sunkara, Joao Monteiro, Krishnamurthy DJ Dvijotham, Torsten Scholak, Nicolas Chapados, Sepideh Kharagani, Sean Hughes, M. Özsu, Siva Reddy, Marco Pedersoli, Yoshua Bengio, Christopher Pal, Issam Laradji, Spandanna Gella, Perouz Taslakian, David Vazquez, and Sai Rajeswar. Bigdocs: An open and permissively-licensed dataset for training multimodal models on document and code tasks, 2024. URL <https://arxiv.org/abs/2412.04626>.
- Eli Schwartz, Leshem Choshen, Joseph Shtok, Sivan Doveh, Leonid Karlinsky, and Assaf Arbelle. NumeroLogic: Number encoding for enhanced LLMs’ numerical reasoning. In Yaser Al-Onaizan, Mohit Bansal, and Yun-Nung Chen (eds.), *Proceedings of the 2024 Conference on Empirical Methods in Natural Language Processing*, pp. 206–212, Miami, Florida, USA, November 2024. Association for Computational Linguistics. doi: 10.18653/v1/2024.emnlp-main.12. URL <https://aclanthology.org/2024.emnlp-main.12/>.
- Nimrod Shabtay, Felipe Maia Polo, Sivan Doveh, Wei Lin, M Jehanzeb Mirza, Leshem Chosen, Mikhail Yurochkin, Yuekai Sun, Assaf Arbelle, Leonid Karlinsky, et al. Livexiv—a multi-modal live benchmark based on arxiv papers content, 2024.
- Oleksii Sidorov, Ronghang Hu, Marcus Rohrbach, and Amanpreet Singh. Textcaps: a dataset for image captioning with reading comprehension, 2020.
- Amanpreet Singh, Vivek Natarajan, Meet Shah, Yu Jiang, Xinlei Chen, Dhruv Batra, Devi Parikh, and Marcus Rohrbach. Towards vqa models that can read, 2019.
- Amanpreet Singh, Guan Pang, Mandy Toh, Jing Huang, Wojciech Galuba, and Tal Hassner. Textocr: Towards large-scale end-to-end reasoning for arbitrary-shaped scene text, 2021.
- Brandon Smock, Rohith Pesala, and Robin Abraham. Pubtables-1m: Towards comprehensive table extraction from unstructured documents. In *Proceedings of the IEEE/CVF Conference on Computer Vision and Pattern Recognition*, pp. 4634–4642, 2022.
- Ryota Tanaka, Kyosuke Nishida, and Sen Yoshida. Visualmrc: Machine reading comprehension on document images, 2021.

- Benny J Tang, Angie Boggust, and Arvind Satyanarayan. Vistext: A benchmark for semantically rich chart captioning, 2023.
- Gemini Team, Petko Georgiev, Ving Ian Lei, Ryan Burnell, Libin Bai, Anmol Gulati, Garrett Tanzer, Damien Vincent, Zhufeng Pan, Shibo Wang, et al. Gemini 1.5: Unlocking multimodal understanding across millions of tokens of context, 2024. URL <https://arxiv.org/abs/2403.05530>.
- Shengbang Tong, Ellis Brown, Penghao Wu, Sanghyun Woo, Manoj Middepogu, Sai Charitha Akula, Jihan Yang, Shusheng Yang, Adithya Iyer, Xichen Pan, Ziteng Wang, Rob Fergus, Yann LeCun, and Saining Xie. Cambrian-1: A fully open, vision-centric exploration of multimodal llms, 2024. URL <https://arxiv.org/abs/2406.16860>.
- Michał Turski, Tomasz Stanisławek, Karol Kaczmarek, Paweł Dyda, and Filip Graliński. Ccpdf: Building a high quality corpus for visually rich documents from web crawl data, 2023a.
- Michał Turski, Tomasz Stanisławek, Karol Kaczmarek, Paweł Dyda, and Filip Graliński. Ccpdf: Building a high quality corpus for visually rich documents from web crawl data, 2023b.
- Shakti N. Wadekar, Abhishek Chaurasia, Aman Chadha, and Eugenio Culurciello. The evolution of multimodal model architectures, 2024. URL <https://arxiv.org/abs/2405.17927>.
- Bryan Wang, Gang Li, Xin Zhou, Zhouong Chen, Tovi Grossman, and Yang Li. Screen2words: Automatic mobile ui summarization with multimodal learning, 2021.
- Dongsheng Wang, Natraj Raman, Mathieu Sibue, Zhiqiang Ma, Petr Babkin, Simerjot Kaur, Yulong Pei, Armineh Nourbakhsh, and Xiaomo Liu. Docllm: A layout-aware generative language model for multimodal document understanding, 2023. URL <https://arxiv.org/abs/2401.00908>.
- Peng Wang, Shuai Bai, Sinan Tan, Shijie Wang, Zhihao Fan, Jinze Bai, Keqin Chen, Xuejing Liu, Jialin Wang, Wenbin Ge, et al. Qwen2-vl: Enhancing vision-language model’s perception of the world at any resolution, 2024.
- Zhengyuan Yang, Yijuan Lu, Jianfeng Wang, Xi Yin, Dinei Florencio, Lijuan Wang, Cha Zhang, Lei Zhang, and Jiebo Luo. Tap: Text-aware pre-training for text-vqa and text-caption, 2021.
- Jiabo Ye, Anwen Hu, Haiyang Xu, Qinghao Ye, Ming Yan, Guohai Xu, Chenliang Li, Junfeng Tian, Qi Qian, Ji Zhang, Qin Jin, Liang He, Xin Alex Lin, and Fei Huang. Ureader: Universal ocr-free visually-situated language understanding with multimodal large language model, 2023. URL <https://arxiv.org/abs/2310.05126>.
- Shukang Yin, Chaoyou Fu, Sirui Zhao, Ke Li, Xing Sun, Tong Xu, and Enhong Chen. A survey on multimodal large language models. *National Science Review*, 11(12), November 2024. ISSN 2053-714X. doi: 10.1093/nsr/nwae403. URL <http://dx.doi.org/10.1093/nsr/nwae403>.
- Ye Yuan, Xiao Liu, Wondimu Dikubab, Hui Liu, Zhilong Ji, Zhongqin Wu, and Xiang Bai. Syntax-aware network for handwritten mathematical expression recognition, 2022.
- Xiang Yue, Yuansheng Ni, Kai Zhang, Tianyu Zheng, Ruoqi Liu, Ge Zhang, Samuel Stevens, Dongfu Jiang, Weiming Ren, Yuxuan Sun, et al. Mmmu: A massive multi-discipline multimodal understanding and reasoning benchmark for expert agi, 2024.
- Christoph Zauner. Implementation and benchmarking of perceptual image hash functions, 2010.
- Xiaohua Zhai, Basil Mustafa, Alexander Kolesnikov, and Lucas Beyer. Sigmoid loss for language image pre-training, 2023.
- Haotian Zhang, Mingfei Gao, Zhe Gan, Philipp Dufter, Nina Wenzel, Forrest Huang, Dhruvi Shah, Xianzhi Du, Bowen Zhang, Yanghao Li, Sam Dodge, Keen You, Zhen Yang, Aleksei Timofeev, Mingze Xu, Hong-You Chen, Jean-Philippe Fauconnier, Zhengfeng Lai, Haoxuan You, Zirui Wang, Afshin Dehghan, Peter Grasch, and Yinfei Yang. Mm1.5: Methods, analysis & insights from multimodal llm fine-tuning, 2024a. URL <https://arxiv.org/abs/2409.20566>.
- Kaichen Zhang, Bo Li, Peiyuan Zhang, Fanyi Pu, Joshua Adrian Cahyono, Kairui Hu, Shuai Liu, Yuanhan Zhang, Jingkang Yang, Chunyuan Li, and Ziwei Liu. Lmms-eval: Reality check on the evaluation of large multimodal models, 2024b. URL <https://arxiv.org/abs/2407.12772>.

- Liang Zhang, Anwen Hu, Haiyang Xu, Ming Yan, Yichen Xu, Qin Jin, Ji Zhang, and Fei Huang. Tinchart: Efficient chart understanding with visual token merging and program-of-thoughts learning, 2024c.
- Yanzhe Zhang, Ruiyi Zhang, Jiuxiang Gu, Yufan Zhou, Nedim Lipka, Diyi Yang, and Tong Sun. Llavar: Enhanced visual instruction tuning for text-rich image understanding, 2023.
- Yilun Zhao, Yunxiang Li, Chenying Li, and Rui Zhang. Multihier: Numerical reasoning over multi hierarchical tabular and textual data, 2022.
- Yilun Zhao, Chen Zhao, Linyong Nan, Zhenting Qi, Wenlin Zhang, Xiangru Tang, Boyu Mi, and Dragomir Radev. Robut: A systematic study of table qa robustness against human-annotated adversarial perturbations, 2023.
- Xinyi Zheng, Doug Burdick, Lucian Popa, Peter Zhong, and Nancy Xin Ru Wang. Global table extractor (gte): A framework for joint table identification and cell structure recognition using visual context. *Winter Conference for Applications in Computer Vision (WACV)*, 2021.
- Xu Zhong, Elaheh ShafieiBavani, and Antonio Jimeno Yepes. Image-based table recognition: data, model, and evaluation, 2020.
- Yongshuo Zong, Ondrej Bohdal, Tingyang Yu, Yongxin Yang, and Timothy Hospedales. Safety fine-tuning at (almost) no cost: A baseline for vision large language models, 2024.

7 APPENDIX

Table 5: A comprehensive overview of document understanding datasets used in Granite Vision.

Datasets	# Images	# QA Pairs
Document QA		
DocFM-VQA	2.4 M	19.9 M
Docmatix (Laurençon et al., 2024a)	565.0 K	3.9 M
synthdog-en (Kim et al., 2022a)	500.0 K	500.0 K
pixmo-docs (Deitke et al., 2024b)	255.4 K	2.3 M
HME100K (Yuan et al., 2022)	74.5 K	74.5 K
Ureader QA (Ye et al., 2023)	72.7 K	370 K
ArxivQA (Li et al., 2024e)	54.4 K	100 K
Ureader KG (Ye et al., 2023)	37.6 K	37.6 K
Tech Book QA	10.4 K	17.8 K
DocVQA (Mathew et al., 2021)	10.2 K	39.5 K
IAM (Marti & Bunke, 2002)	5.7 K	5.7 K
Business Document QA	3.3 K	7.8 K
Visualmrc (Tanaka et al., 2021)	3.0 K	12 K
Chart QA		
Unichart (Masry et al., 2023)	611.0 K	6.9 M
Tinychart (Zhang et al., 2024c)	606.0 K	4.5 M
DocFM-VQA-Charts	548.7 K	5.5 M
Dvqa (Kafle et al., 2018)	200.0 K	2.3 M
PlotQA (Methani et al., 2020)	157.0 K	20.2 M
FigureQA (Kahou et al., 2017)	100.0 K	1.3 M
DocFM-VQA-AugChartQA	35.1 K	294.2 K
Chart2Text (Obeid & Hoque, 2020)	27.0 K	30.0 K
ChartQA (Masry et al., 2022)	18.3 K	28.3 K
Vistext (Tang et al., 2023)	9.9 K	9.9 K
Infographics QA		
Infographic VQA (Mathew et al., 2022)	8.5 K	35.7 K
Table QA		
RoBUT-wikiSQL (Zhao et al., 2023)	75.0 K	86.2 K
RoBUT-WTQ (Zhao et al., 2023)	38.0 K	44.1 K
tabmwp (Lu et al., 2022)	22.7 K	23 K
RoBUT-SQA (Zhao et al., 2023)	8.5 K	34.1 K
MultiHiertt (Zhao et al., 2022)	7.6 K	7.8 K
Finqa (Chen et al., 2021)	5.3 K	6.25 K
Hitab (Cheng et al., 2022)	2.5 K	7.8 K
Diagram QA		
TQA (Kembhavi et al., 2017)	27.3 K	29.8 K
DocFM-VQA-Flowcharts	16.6 K	74.6 K
AI2D GPT4V (Li et al., 2024b)	4.9 K	4.9 K
AI2D InternVL (Li et al., 2024b)	3.2 K	12.4 K
AI2D (Kembhavi et al., 2016)	2.4 K	7.5 K
Diagram Image2Text ⁷	0.3 K	0.3 K
Reasoning / Captioning		
DocFM Visual Cue & Captioning	1.2 M	2.1 M
Textcaps (Sidorov et al., 2020)	22.0 K	22.0 K
DocReason ⁸	8.7 K	25.8 K

Continued on next page

Table 5 – Continued from previous page

Datasets	# Images	# QA Pairs
Grounding / Text Localization		
Multi-grained Text Localization (Hu et al., 2024b)	1.0 M	1.0 M
DocFM Rule Based Grounding	190 K	534.4 K
KVP10K (Naparstek et al., 2024)	8.0 K	8.0 K
Scene Text		
K12 Printing (Li et al., 2024d)	256.6 K	256.6 K
OCR-VQA (Mishra et al., 2019)	165.7 K	801.6 K
TextOCR (Singh et al., 2021)	25.1 K	25.1 K
Ureader CAP (Ye et al., 2023)	22.0 K	91.4 K
TextVQA (Singh et al., 2019)	22.0 K	34.6 K
Llavar (Zhang et al., 2023)	19.8 K	43.2 K
ST-VQA (Biten et al., 2019)	16.4 K	22 K
RenderedText ⁹	10.0 K	10.0 K
IIIT5K (Mishra et al., 2012)	2.0 K	2.0 K
UI Screen / Code		
Datikz-v2 ¹⁰	94.4 K	94.4 K
Datikz (Belouadi et al., 2023)	47.9 K	48.2 K
screenqa (Hsiao et al., 2022)	33.2 K	80.8 K
screen2words (Wang et al., 2021)	15.7 K	15.7 K
websight (Laurençon et al., 2024)	10.0 K	10.0 K
Omniact (Kapoor et al., 2024)	4.9 K	0.13 K
Structure Parsing		
OCR-CC (Yang et al., 2021)	1.0 M	1.0 M
CCpdf (Turski et al., 2023b)	937.8 K	937.8 K
PubTables (Smock et al., 2022)	569.3 K	569.3 K
Chart2Table	550.4 K	550.4 K
TURL (Deng et al., 2022)	200.0 K	200.0 K
PubTabNet (Zhong et al., 2020)	199.8 K	199.8 K
RVL-CDIP (Harley et al., 2015)	159.4 K	159.4 K
DUE (Borchmann et al., 2021)	104.5 K	1.6 M
FinTabNet (Zheng et al., 2021)	98.9 K	98.9 K

⁷https://huggingface.co/datasets/Kamizuru00/diagram_image_to_text⁸<https://huggingface.co/datasets/mPLUG/DocReason25K>⁹<https://huggingface.co/datasets/wendlerc/RenderedText>¹⁰<https://huggingface.co/datasets/nllg/datikz-v2>

8 CONTRIBUTIONS AND ACKNOWLEDGMENTS

Authors (alphabetical order):

Granite Vision Technical Leadership:

Assaf Arbelle, Leonid Karlinsky, Peter Staar, Rogerio Feris, Tal Drory

Project Management:

Abraham Daniels

Core Contributors:

Ahmed Nassar, Amit Alfassi, Bo Wu, Eli Schwartz, Dhiraj Joshi, Jovana Kondic, Nimrod Shabtay, Pengyuan Li, Roei Herzig, Shafiq Abedin, Shaked Perek, Sivan Harary, Udi Barzelay

Contributors:

Adi Raz Goldfarb, Aude Oliva, Ben Wieles, Bishwaranjan Bhattacharjee, Brandon Huang, Christoph Auer, Dan Gutfreund, David Beymer, David Wood, Hilde Kuehne, Jacob Hansen, Joseph Shtok, Ken Wong, Luis Angel Bathen, Mayank Mishra, Maksym Lysak, Michele Dolfi, Mikhail Yurochkin, Nikolaos Livathinos, Nimrod Harel, Ophir Azulai, Oshri Naparstek, Rafael Teixeira de Lima, Rameswar Panda, Sivan Doveh, Shubham Gupta, Subhro Das, Syed Zawad, Yusik Kim, Zexue He

Platform:

Alexander Brooks, Gabe Goodhart

Product Management:

Anita Govindjee, Derek Leist, Ibrahim Ibrahim

IBM Research Leadership:

Aya Soffer, David Cox, Kate Soule, Luis Lastras, Nirmal Desai, Shila Ofek-koifman, Sriram Raghavan, Tanveer Syeda-Mahmood

Acknowledgments:

We would like to acknowledge Amy Angelini, Bob Calio, Brian Belgodere, Dakshi Agrawal, Heiko Ludwig, Hendrik Strobel, John Smith, Kim Martineau, Kush Varshney, Mauro Martino, Petros Zerfos, Ray Rose, and Sandeep Gopisetty. We would also like to acknowledge the support from IBM Research AI and the MIT-IBM Watson AI lab.